A study of the structural phase transformation and superconductivity in HfV$_2$

M J Parsons†, P J Brown†‡, J Crangle§, K-U Neumann†, B Ouladdiaf‡,
T J Smith†, N K Zayer† and K R A Ziebeck†‖

† Department of Physics, Loughborough University, Leicestershire LE11 3TU, UK
‡ Institut Laue–Langevin, BP156 Grenoble 38042, France
§ Department of Physics, University of Sheffield, Sheffield S3 7RH, UK

Abstract. Specific heat and magnetization measurements on the hard superconductor Hf V$_2$ confirm the presence of a structural phase transformation at 117 K and a superconducting transition temperature of 9 K. Above 117 K the compound has the cubic Laves phase C15 structure. High-resolution neutron powder diffraction measurements reveal that below 117 K there is a mixed phase structure consisting predominantly of an orthorhombic component together with a cubic untransformed part. Both of these phases superconduct and their critical temperatures are similar, if not identical. In the normal state the magnetic properties are consistent with those expected for a Pauli paramagnet in which the Fermi level lies just below a high peak in the density of states. These conclusions are supported by band-structure calculations carried out using the linear muffin-tin orbital (LMTO) approximation.

1. Introduction

Many traditional type-II superconductors which contain transition elements also show a lattice instability, often resulting in a structural phase transition (Testardi 1975). Usually the phase transition occurs at a temperature T_m higher than that of the transition, T_c, to a superconducting state. Thus the superconductivity occurs in the low-temperature phase in which the lattice becomes more rigid. However, as a result of strong electron–phonon coupling the superconducting transition at T_c is thought to be significantly influenced by the lattice instability. This feature has been extensively studied in compounds with the A15 structure, for example V$_3$Si, which undergoes a transition to a tetragonal variant at low temperatures (Battermann and Barrett 1966). This transition is martensitic and is thought to be due to a band Jahn–Teller interaction (Labbe and Friedel 1966a, b). X-ray diffraction measurements have shown that the deviation of the axial ratio c/a from unity increases below T_m and saturates at the superconducting transition temperature T_c, suggesting that the onset of superconductivity inhibits further distortion. Structural phase transitions have also been observed in the normal phase of superconductors having the cubic C15 Laves phase structure (Lawson and Zachariasen 1972). Of those Laves phase compounds which exhibit superconductivity, HfV$_2$ has one of the highest transition temperatures, namely 9 K (Rapp and Vieland 1971). From a combined analysis of specific heat and susceptibility data, Hafstrom *et al* (1978) estimated the temperature dependence of the mean geometric

‖ Author to whom any correspondence should be addressed.

frequency of the phonon spectrum $\langle\omega\rangle$ for $Ta_xHf_{1-x}V_2$. Their analysis indicated a decrease in $\langle\omega\rangle$ and therefore a softening of the lattice before the occurrence of the phase transition, which in the stoichiometric compound HfV_2 occurs at 117 K. Ultrasonic measurements indicate a softening of the elastic constants which takes place over a wide temperature range (Luthi *et al* 1985). Between room temperature and 117 K, C_{44} decreases by 12% whereas C', which is given by $\frac{1}{2}(C_{11} - C_{12})$, softens by 45%. A precise knowledge of the ground-state crystallographic structure is fundamental to understanding the mechanisms involved in the transition.

Although HfV_2 has the cubic Laves phase C15 structure above 117 K, below this temperature it transforms to a phase of lower symmetry which has been variously reported, on the basis of limited x-ray measurements, as being either tetragonal (Finkel and Pushkarev 1980, Chu and Pope 1992) or orthorhombic (Lawson and Zachariasen 1972). As in the case of the A15 compounds, the phase transition is reported to be diffusionless, and reversible with a negligible change in volume (Hafstrom *et al* 1978, Luthi *et al* 1985, Chu *et al* 1996). High-resolution powder neutron diffraction measurements have therefore been undertaken to determine the low-temperature crystallographic structure. Although the coherent nuclear scattering amplitude of V for thermal neutrons is small, that of Hf is not, and so the measurements should enable the low-temperature crystallographic structure to be established and the ambiguity resolved. X-ray, specific heat and magnetization measurements were also carried out to characterize the sample and to ensure that it had the properties reported previously for HfV_2. For the normal state, the results of a band-structure calculation carried out using the linear muffin-tin orbital (LMTO) approximation have been compared with the properties determined experimentally.

2. Physical properties

At room temperature, HfV_2 crystallizes in the cubic Laves structure with space group $Fd\bar{3}m$ and a lattice parameter of 7.366 Å. The Hf atoms form a diamond structure in the interstices of which the interconnecting V tetrahedra are located. In this structure the nearest-neighbour Hf distance is $a\sqrt{3}/4 = 3.189$ Å. The nearest-neighbour vanadium distance is $a\sqrt{2}/4 = 2.604$ Å. The influence of alloying on both T_c and T_m has been investigated in systems in which either the Hf or the V sites have been systematically substituted for with other transition elements (Hafstrom *et al* 1978, Inoue *et al* 1979). The results of these investigations reveal an inverse relationship between T_c and T_m; if T_c decreases then T_m increases and vice versa (Inoue and Tachikawa 1977). Measurement of the pressure dependence of the resistivity $\rho(T)$ in $(ZrHf)V_2$ and $(TaHf)V_2$ systems indicate a rise in T_c with increasing pressure but a decrease in T_m (Smith *et al* 1973). The specific heat anomaly associated with the structural phase transition occurs over a finite temperature range (Chu *et al* 1996). There is hysteresis in some of the physical parameters which change at T_m, such as the resistivity (Luthi *et al* 1985).

An enhanced electronic contribution to the specific heat has been reported, and within the superconducting region the specific heat varies as T^3. The height of the specific heat jump ΔC at T_c is also seen to be larger than the 1.43 predicted by BCS theory. Such observations have led to HfV_2 being classed among the heavy-fermion materials and, furthermore, as a strong-coupling superconductor (Luthi *et al* 1985, Chu *et al* 1996, Kishimoto *et al* 1992) in which the gap is anisotropic, vanishing at points on the Fermi surface. Below T_c, the thermal conductivity decreases as expected but the rate of decrease becomes less pronounced at 4 K. This change in conductivity was explained by assuming that the electronic contribution decreases and the phonon contribution increases (Luthi *et al* 1985). However, the results

presented here suggest that the mechanism may be more complicated. In the normal state, the electrical resistivity has a tendency to saturate, approaching the Mott limit in which the mean free path becomes of atomic size. Susceptibility, specific heat and Knight shift measurements all suggest that there is a sharp peak in the density of states close to the Fermi level.

3. Experimental procedure

A 30 g ingot of HfV$_2$ was prepared by the repeated melting of the appropriate quantities of spectrographically pure (5N) starting elements in an argon arc furnace. The weight loss after melting was less than 0.1%. A 1.5 g sample was spark eroded from the ingot and one side polished for the heat capacity measurements. The remainder was crushed to a particle size of less than 250 μm before being sealed under a reduced atmosphere of argon in a quartz tube. Homogenization of the specimen was carried out by heating at 1000 °C for 48 hours, after which the specimen was quenched into cold water. The temperature at which the sample was annealed was the same as that employed in the majority of previous investigations on HfV$_2$. X-ray powder diffraction measurements confirmed that the specimen had the cubic C15 (CuMg$_2$) Laves phase structure with lattice parameter $a = 7.386$ Å, with space group $Fd\bar{3}m$. No secondary phases were apparent.

The specific heat was measured within the temperature range from 2 K to 150 K using a modified adiabatic heat pulse calorimeter. Magnetizations were measured on samples weighing about 200 mg using a SQUID magnetometer, in accurately controlled fields of between 1 mT and ± 5 T at temperatures between 2 K and 300 K. Demagnetizing corrections were applied to the values of the externally applied field.

Powder neutron diffraction measurements were undertaken at the Institut Laue–Langevin in Grenoble using the diffractometers D1B and D2B. D1B was chosen because of its wide angular range and facility for rapid data collection over a wide temperature range; and D2B for its high resolution. The neutron wavelength was either 2.3 Å (D1B) or 2.4 Å (D2B). The specimen was contained in a thin-walled vanadium tube of diameter 7 mm placed in a helium-flow cryostat. The scattering angles were in steps of: $0.2°$ from 5 to $85°$ (D1B); $0.05°$ from 2 to $160°$ (D2B).

4. Results

4.1. Magnetization

4.1.1. Observations for weak fields. That a superconducting state does indeed occur in HfV$_2$ at low temperatures is demonstrated in figure 1. The magnetization was measured at temperatures increasing in steps of 0.5 K, from $T = 2.0$ K to $T = 15.0$ K, in a steady applied field of 2 mT. Up to $T = 8.5$ K, the specimen was strongly diamagnetic; it was slightly diamagnetic at $T = 9.0$ K and weakly paramagnetic at higher temperatures. This is an observation of a conventional Meissner effect, corresponding to a value of T_c slightly above $T = 9.0$ K and below $T = 9.5$ K.

In the perfectly diamagnetic superconducting state, all magnetic flux is excluded from the specimen. The calculated mass susceptibility for an ideal diamagnet is $\chi = -1/(\mu_0\rho)$ in SI units. Taking the density of HfV$_2$ as $\rho = 9300$ SI (the crystallographic value) and the permeability of free space as $\mu_0 = 4\pi \times 10^{-7}$ gives the expected ideal value of $\chi = -8557 \times 10^{-2}$ SI. The most negative experimental value at $T = 2$ K is $\chi = -9071 \times 10^{-2}$ SI, some 6% higher than it would be in the ideal case with all of
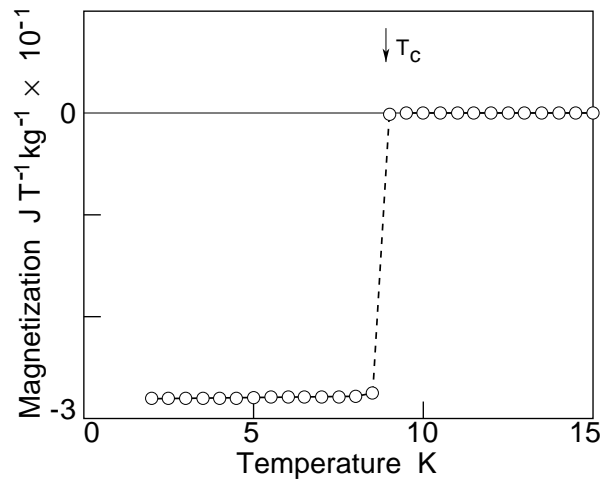
Figure 1. The magnetization of HfV_2 measured in a field of 2 mT at temperatures around T_c.
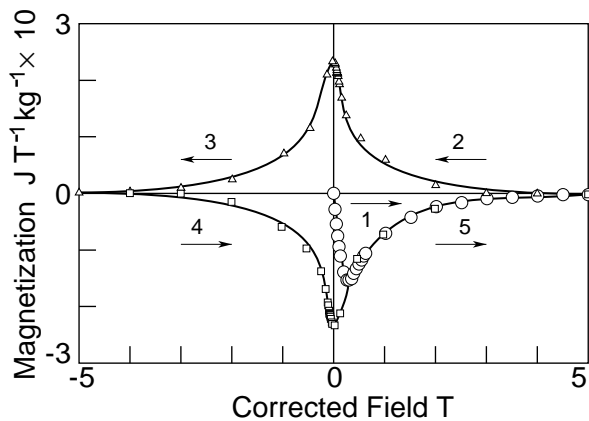

Figure 2. The hysteresis loop of HfV_2 at $T = 5$ K after cooling from $T = 300$ K in zero field.

the specimen superconducting. This 6% difference can be accounted for as the probable error in assuming the density of the sample to be the crystallographic value, rather than the reduced density of a packed powder sample. It is thus reasonable to conclude that at $T = 2$ K virtually all of the sample is superconducting when the applied field is of the order of 2 mT. The measurement was repeated at temperatures up to $T = 10.0$ K in steps of 0.5 K. The highest diamagnetic susceptibility decreased very slowly with increasing temperature, so at $T = 8.0$ K its value was 5.4% higher than the ideal value; at $T = 8.5$ K it was 4.7% higher than the ideal value. At $T = 9.0$ K, it had fallen catastrophically. At higher temperatures the susceptibility was no longer diamagnetic. Thus, within the error of a few per cent arising from the uncertain density of the powder specimen, the Meissner fraction of the mixed-phase sample is the same at all temperatures between $T = 2$ K and $T = 8.5$ K; that is, the sample is completely superconducting with both phases contributing. Any difference in T_c between the two phases would have to take place between $T = 8.5$ K and $T = 9$ K. As shown in figure 5(b), the electronic specific heat capacity shows no
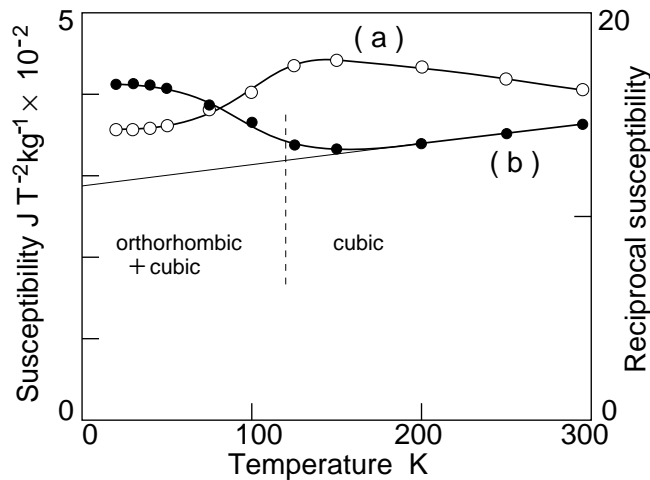
Figure 3. The susceptibility (a) and reciprocal susceptibility (b) of HfV$_2$ as a function of temperature in the paramagnetic state.

evidence of a maximum associated with at least 30% of the sample having superconducting transition temperatures differing by more than 0.5 K. A smaller difference would not be detectable.

4.1.2. Hysteresis at temperatures below T_c. For the measurements illustrated in figure 2, the specimen was first cooled from $T = 300$ K to $T = 5$ K in zero magnetic field. While a steady temperature of $T = 5$ K was maintained, the field was taken in the direction of the arrows and in the sequence of the numbers on the diagram. Demagnetizing corrections were applied to the data. Similar hysteresis loops were observed at other temperatures below T_c until by 9 K they had almost disappeared. Such loops are well known in type-II hard superconductors.

4.1.3. Paramagnetism at temperatures above T_c. At temperatures above T_c, HfV$_2$ is paramagnetic. The susceptibility depends on temperature, having a broad maximum at $T = 150$ K (figure 3 (curve (a))). The reciprocal of the susceptibility appears to depend linearly but weakly on temperature above $T = 200$ K (see figure 3 (curve (b))). The broken line indicates the temperature of the structural phase change.

4.2. Specific heat

The specific heat C_p of HfV$_2$ as a function of temperature between $T = 100$ K and $T = 135$ K is shown in figure 4. A distinct anomaly is observed, with a maximum occurring at $T_M = 117$ K where the structural phase transition takes place. The height of the anomaly, $\Delta C \sim 160$ J K^{-1} mol^{-1}, and the narrow width of the peak (full width about 1 K at half-height) are noteworthy. The shape of the specific heat peak appears to be of λ-type, agreeing with the earlier studies.

In the region of the superconducting transition, the specific heat is seen to rise to a maximum at $T_C = 9$ K. In order to compare the results of the present specific heat measurements with those reported earlier (Luthi *et al* 1985, Chu *et al* 1996, Kishimoto *et al*
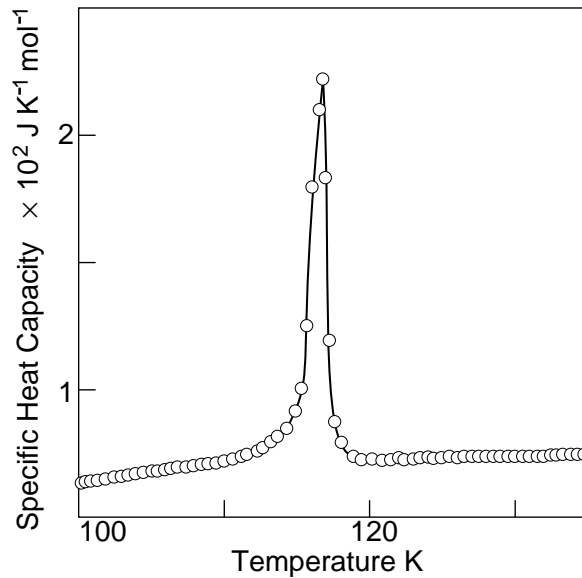
Figure 4. The specific heat of HfV_2 around the structural transformation.

1992), the same functional form was used to analyse the data. The data above T_c in the normal state were analysed assuming the following contributions:

$$C_p = \gamma T + \beta T^3 + \alpha T^5 + \delta T^7.$$

The term linear in T gives the electronic Sommerfeld coefficient and the remainder is attributed to lattice vibrations. The fit was performed using the constraint that the entropies of the normal and superconducting states should balance:

$$s_n = \int_0^{T_C} C_n/T \ dT = \int_0^{T_C} C_s/T \ dT = s_s$$

where C_n is the specific heat given by the fit and C_s the superconducting specific heat measured by experiment. The entropies calculated by such a relationship are consistent to within 0.5%. The coefficients for this fit, given in table 1, agree with those reported earlier (Kishimoto *et al* 1992, Luthi *et al* 1985, Rapp and Vieland 1971) as does the Debye temperature. The value obtained for the coefficient linear in temperature, $\gamma = 52$ mJ K^{-2} mol^{-1}, is significantly larger than that expected for a normal metal and suggests a large density of electronic states at the Fermi level, a result consistent with band-structure calculations carried out during the course of the present work. This observation has led to HfV_2 being classed at the lower end of the heavy-fermion category.

Using $C_p = \gamma T + \beta T^3 + \alpha T^5 + \delta T^7$, as described above, the phonon contribution to the observed specific heat was subtracted to leave only the electronic part C_e (figure 5(a)). The transition temperature T_c and the jump ΔC in the specific heat can be seen clearly. The electronic specific heat is approximately proportional to the cube of the temperature below T_c (figure 5(b)). These results agree with results previously published (Rapp and Vieland 1971, Hafstrom *et al* 1978, Luthi *et al* 1985). They verify the nature of the system as having strong electron–phonon coupling, and that the quality of the sample was good.

Table 1. Parameters derived from the specific heat measurements.

T_M (K)	T_C (K)	γ (mJ K^{-2} mol^{-1})	β	α $\times 10^{-3}$	δ $\times 10^{-6}$	Θ_D (K)	$\Delta C/\gamma T_C$	Reference
117	9.1	51.6	1.23	−4.161	3.989	165	1.85	a
—	9.2	47.7	1.13	−2.760	2.400	151	2.0	b
118	9	58.1	1.17	−4.075	8.380	170	1.9	c
—	8.4	19.0	—	—	—	190	1.7	d

[a] This work.
[b] Kishimoto *et al* (1992).
[c] Luthi *et al* (1985).
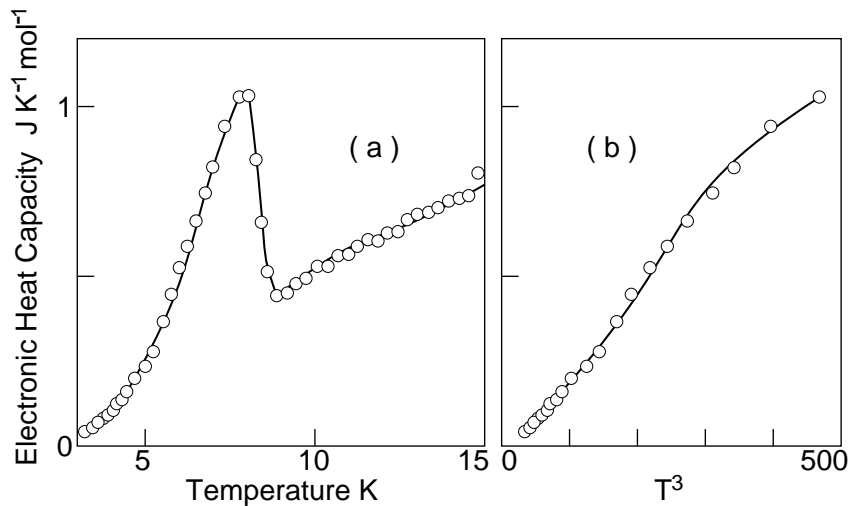[d] Rapp and Vieland (1971).

Figure 5. The electronic contribution to the specific heat of HfV₂ near the superconducting transition, plotted (a) against temperature and (b) against the cube of the temperature.

4.3. Neutron scattering

At $T = 125$ K, nine distinct Bragg peaks were observed (figure 6) over the angular range of 2θ between $2°$ and $160°$. These peaks were indexed on a face-centred cubic lattice, consistent with the sample being of single phase; profile refinement confirmed the cubic Laves phase structure. Since the nuclear coherent scattering amplitude of vanadium is small, the refinement was essentially carried out using only the hafnium atoms. In figures 6 and 7, each upper graph shows the experimental data; the marks on the upper boundary show the synthesis for the structure derived; the lower graphs plot the difference between the calculated and the actual intensities. Details of the structural parameters obtained from the refinement are given in the first column of table 2. They agree with those reported earlier by Lawson and Zachariasen (1972) for this temperature. A statistical chi-squared test was applied to the fit, defined by

$$\chi^2 = \sum \frac{(F_{obs} - F_{calc})^2}{(\sigma F_{obs})^2} \Big/ (N_{obs} - N_{par})$$
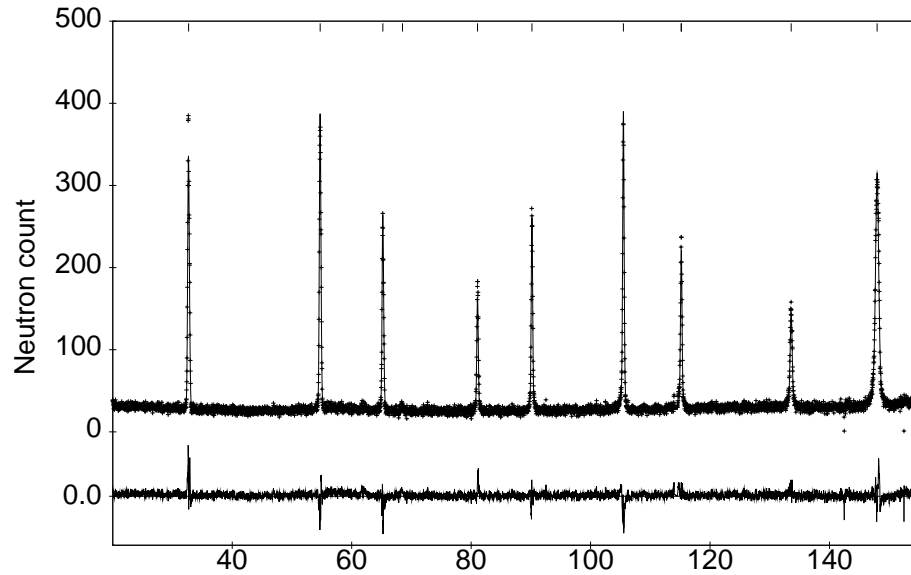
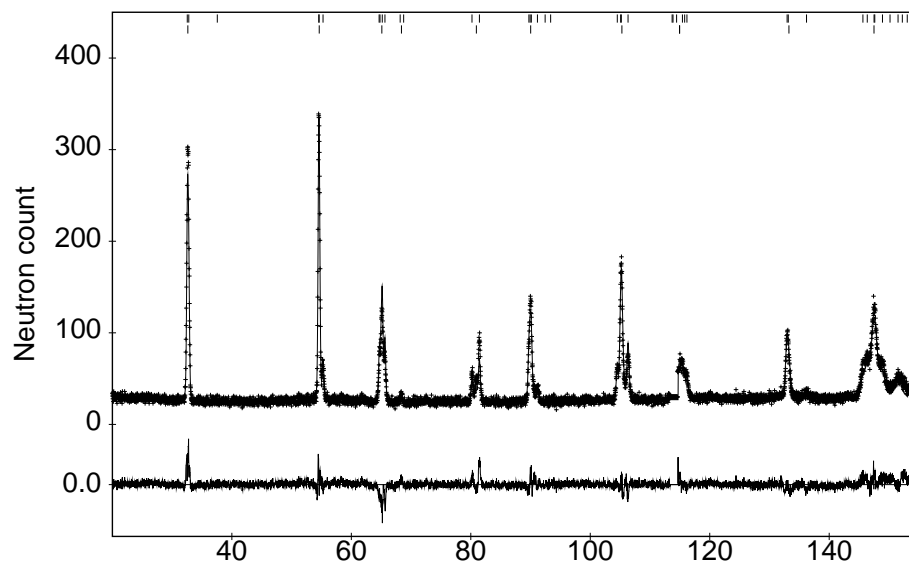**Figure 6.** The neutron powder diffraction pattern of HfV$_2$ at $T = 125$ K.

Figure 7. The neutron powder diffraction pattern of HfV$_2$ at $T = 30$ K.

(N_{obs} is the number of observations and N_{par} is the number of parameters). The result, shown in the table, was entirely satisfactory.

On cooling to $T = 30$ K, the diffraction pattern became more complicated (figure 7). Some of the original cubic peaks split, but no new peaks, remote from the original cubic reflections, appeared. The splitting of the Bragg reflections suggests that the cubic symmetry is lost, while the absence of new peaks suggests that the translational symmetry is unaltered. The list of non-cubic, non-isomorphic subgroups of the space group includes the space

Table 2. Crystallographic parameters of HfV$_2$.

$T = 125$ K	$T = 30$ K	
Cubic Laves ($Fd\overline{3}m$)	Orthorhombic ($Imma$)	Cubic ($Fd\overline{3}m$)
Hf 8(c) 0 0 0	4(e) 0 1/4 z; $z = 0.1126(9)$	8(c) 0 0 0
V 16(d) 5/8 5/8 5/8	4(b) 0 0 1/2	16(d) 5/8 5/8 5/8
V	4(d) 1/4 1/4 1/4	
100%	$67 \pm 1\%$	$33 \pm 1\%$
$a = 7.3545(2)$ Å	$a = 5.2177(6)$ Å	$a = 7.3894(3)$ Å
	$b = 5.1708(4)$ Å	
	$c = 7.4489(9)$ Å	
$\chi^2 = 1.9$	$\chi^2 = 2.0$	

groups $I4_1/amd$ and $R\overline{3}m$. However, it is apparent from the number of reflections and their relative intensities that the low-temperature phase is not tetragonal or rhombohedral; nor is it totally orthorhombic as had been previously reported by Lawson and Zachariasen (1972); nor is it totally tetragonal as reported previously by Finkel and Pushkarev (1980) and by Chu and Pope (1992). Inspection of the position of the peaks and in particular what was formerly (220), which splits into two parts but with an intensity ratio of approximately 10:1, suggests that the structure transforms partially into an orthorhombic phase having the cell parameters shown in table 2. These values agree well with those proposed by Lawson and Zachariasen (1972), if the a- and b-axes are transposed. However, the space group was found to be $Imma$ and not $Imm2$ as proposed by Lawson and Zachariasen (1972). The atomic positions in the transformed orthorhombic structure are given in table 2, from which it may be seen that the hafnium atoms no longer occupy special positions. An initial refinement was performed using these parameters and the space group $Imma$, which is a non-isomorphic subgroup of $I4_1/amd$. This structure accounted for the majority of the peaks and did not produce any additional ones. The refinement was repeated, this time allowing the z-parameter of the Hf atoms to vary. This led to a significant improvement. However, there still remained some peaks which were not accounted for. For example, the cubic (400) reflection splits into three peaks and clearly one of them was not predicted by the model. The additional peak occurs at a position close to that expected for the (400) reflection assuming the cubic cell parameter.

Thus it appears that not all of the sample transforms to the phase having the lower symmetry. Similar behaviour has been observed for the related compound ZrV$_2$ by Moncton (1973). Therefore a refinement was carried out assuming two phases to be present, one with orthorhombic symmetry, the other being the original high-temperature cubic Laves structure. The result of the refinement agrees well with observation, again with an entirely satisfactory result in the chi-squared test. The parameters obtained from the refinement are shown in the second and third columns of table 2. The calculated line positions for the two phases are marked separately at the top edge of figure 7.

The results show that at $T = 30$ K the sample contains $67 \pm 1\%$ of the orthorhombic phase together with $33 \pm 1\%$ of untransformed cubic Laves phase. The amount of cubic phase probably depends on the thermal history of the actual sample and possibly on temperature. This might well explain some of the discrepancies in the results obtained by different groups of workers.

5. Discussion

In the normal state, the thermal variation of the specific heat is dominated by the structural phase transition at 117 K. However, there is no feature in the temperature variation of the susceptibility at or near $T = 117$ K. The nearest feature is a broad maximum centred around $T = 150$ K, the temperature of which is independent of the applied field. Away from the transition, above approximately 200 K, the inverse susceptibility increases linearly and weakly with temperature. Both the magnitude and the thermal variation of the susceptibility are consistent with that expected for a transition metal paramagnet. Self-consistent band-structure calculations using the LMTO approximation indicate a peak in the density of d states in the vicinity of the Fermi level. The calculated density of states at the Fermi level is 12.4 states eV^{-1}/atom. These calculations are in good agreement with those recently reported in which the Fermi level lies in a minimum just below a peak in the density of states (Jarlborg and Freeman 1980, Ormec *et al* 1996). The paramagnetic susceptibility is then expected to have two main contributions, namely a Pauli susceptibility $\chi_P(T)$ and an orbital susceptibility $\chi_{orb}(T)$, arising from partially occupied sub-bands. Thus if the diamagnetic susceptibility is neglected, the observed susceptibility is

$$\chi(T) = \chi_{orb}(T) + \chi_P(T).$$

Typical numerical estimates of χ_{orb} for transition metals are of order one molar SI unit—for example 2.10 molar SI units for vanadium (Collings and Ho 1971)—which would suggest an expected value of 1×10^{-2} mass SI units for HfV$_2$.

For non-interacting electrons, $\chi_P(0)$ is proportional to the bare electronic density of states, as is the Sommerfeld coefficient $\gamma(0)$. Therefore,

$$\chi_P = 13.714\gamma = n(\epsilon_F)/0.212$$

where χ_P, γ and $n(\epsilon_F)$ are in the appropriate molar SI units. Using a molecular weight of 280.5, the measured unrenormalized specific heat coefficient yields a value for χ_P of 2.52×10^{-2} mass SI units, in reasonable agreement with observation. The corresponding density of states is 10.9 states eV^{-1}/atom. Thus the observed magnitude of the normal-state susceptibility and Sommerfeld coefficient are self-consistent and are in reasonable agreement with those values derived from the calculated electronic density of states. In general the appreciable d bandwidth renders the Pauli susceptibility insensitive to thermal change above this temperature region. From the calculated band structure it is clear that there is insufficient structure to provide the observed temperature dependence for χ_P. To account for the thermal variation, many-body effects need to be considered. Clearly the observed quantities include the influence of electron–electron and electron–phonon interactions not included in the band-structure calculations. Inclusion of many-body effects through models such as that proposed by McMillan (1968) has been discussed by Hafstrom *et al* (1978) whose susceptibility and specific heat results agree well with those reported here. The thermal variation of the susceptibility above 200 K may be ascribed to spin fluctuations. The neutron diffraction measurements that were also made over a wide temperature range on the D1B spectrometer confirm the absence of any cooperative magnetic state at low temperatures.

The magnetization measurements below 9 K confirm that HfV$_2$ is a type-II hard superconductor. Between $T = 2$ K and $T = 8.5$ K a complete Meissner effect was found, involving the whole of the sample. It is clear from the neutron diffraction measurements that significant amounts of the two crystal structures were present throughout the superconducting range. Thus both the cubic and the orthorhombic states must be superconducting. However,

there was no evidence found of there being two appreciably separate superconducting phase transitions associated with these two components. The relatively high jump in the specific heat at T_c has led to HfV$_2$ being classed as a strong-coupling superconductor. However, the peak in the specific heat is relatively broad, with a T^3-variation only occurring below 0.8 T_c. On the basis of these results, the possibility of there being two very close superconducting transitions cannot be ruled out. Since the system is in the strong-coupling limit, T_c depends on the mean geometric frequency of the phonon spectrum $\langle \omega \rangle$ rather than a particular phonon frequency. Thus $\langle \omega \rangle$ is unlikely to be very different for the two crystallographic structures.

From the position of the diffraction peaks in the low-temperature phase, it appears that the structural phase transition is driven by a $q = 0$ mode, whereas the superconductivity is expected to be determined primarily by the high-frequency phonon modes. Consequently the thermal variation of the elastic constants as indicated by the ultrasonic measurements of Luthi *et al* (1985) is essentially pertinent only to the structural phase transition. For a quantitative understanding of the superconducting transition, a knowledge of the high-frequency phonon modes is required, together with the electron–phonon matrix elements. Until this information is available it will not be possible to understand fully the interdependence between the structural phase transition and the superconducting transition.

No Bragg peaks of magnetic origin were found in the neutron powder patterns, nor any magnetic diffuse scattering. No evidence of any magnetic long-range order was found as a result of the SQUID measurements.

6. Conclusions

Specific heat measurements have confirmed the strong-coupling nature of HfV$_2$ and the occurrence of a structural phase transition at $T = 117$ K. The normal-state properties are consistent with there being a high electron density of states in the vicinity of the Fermi energy. Calculation of the band structure using the LMTO approach produces a density of states which is in reasonable agreement with that estimated from the magnetic susceptibility and Sommerfeld coefficient. High-resolution neutron diffraction measurements below $T = 117$ K did not show any coherent magnetic scattering, a result consistent with the prediction that local moments on vanadium only occur for V-to-V nearest-neighbour distances greater than 2.85 Å (Hattox *et al* 1973). Thus the temperature variation of the uniform paramagnetic susceptibility is most probably the result of many-body effects. Neutron diffraction measurements have enabled the low-temperature structure to be determined and the previous ambiguity based on limited x-ray measurements to be resolved. The two crystal structures present below $T = 117$ K both superconduct and no difference between their superconducting transition temperatures was found.

References

Battermann B W and Barrett C S 1966 *Phys. Rev.* **145** 296
Chu F, Chen Z W, Fuller C J, Liu C I and Mihalisin T J 1996 *J. Appl. Phys.* **79** 6405
Chu F and Pope D P 1992 *Scr. Metall.* **26** 399
Collings E W and Ho J C 1971 *Phys. Rev.* B **4** 349
Finkel V A and Pushkarev E A 1980 *Sov. Phys.–JETP* **51** 422
Hafstrom J W, Knapp G S and Aldred A T 1978 *Phys. Rev.* B **17** 2892
Hattox T M, Conklin J B Jr, Slater J C and Trickey S B J 1973 *J. Phys. Chem. Solids* **34** 1627
Inoue K, Kuroda T and Tachikawa K 1979 *IEEE Trans. Magn.* **15** 635
Inoue K and Tachikawa K 1977 *IEEE Trans. Magn.* **13** 84
Jarlborg T and Freeman A J 1980 *Phys. Rev.* B **22** 2332

Kishimoto Y, Shibata N, Ohno T, Kitaoka Y, Asayama K, Amaya K and Kanashiro T 1992 *J. Phys. Soc. Japan* **61** 696

Labbe J and Friedel J 1966a *J. Physique* **27** 153

——1996b *J. Physique* **27** 303

Lawson A C and Zachariasen W H 1972 *Phys. Lett.* **38A** 1

Luthi B, Herrmann M, Assmus W, Schmidt H, Rietschel H, Wuhl H, Gottsick U, Sparn G and Steglich F 1985 *Z. Phys.* B **60** 387

McMillan W L 1968 *Phys. Rev.* **167** 331

Moncton D E 1973 *Solid State Commun.* **13** 1779

Ormec A, Chu F, Wills J M, Mitchell T E, Albers R C, Thoma D J and Chen S P 1996 *Phys. Rev.* B **54** 12 753

Rapp Ö and Vieland L J 1971 *Phys. Lett.* **36A** 369

Smith T F, Shelton R N and Lawson A C 1973 *J. Phys. F: Met. Phys.* **3** 2157

Testardi L R 1975 *Rev. Mod. Phys.* **47** 637